

Hexatic phase in the two-dimensional Gaussian-core model

Santi Prestipino¹ [*], Franz Saija² [†], and Paolo V. Giaquinta¹ [‡]

¹ *Università degli Studi di Messina, Dipartimento di Fisica, Contrada Papardo, I-98166 Messina, Italy*

² *CNR-IPCF, Viale Ferdinando Stagno d'Alcontres 37, 98158 Messina, Italy*

(Dated: February 17, 2022)

We present a Monte Carlo simulation study of the phase behavior of two-dimensional classical particles repelling each other through an isotropic Gaussian potential. As in the analogous three-dimensional case, a reentrant-melting transition occurs upon compression for not too high temperatures, along with a spectrum of water-like anomalies in the fluid phase. However, in two dimensions melting is a continuous two-stage transition, with an intermediate hexatic phase which becomes increasingly more definite as pressure grows. All available evidence supports the Kosterlitz-Thouless-Halperin-Nelson-Young scenario for this melting transition. We expect that such a phenomenology can be checked in confined monolayers of charge-stabilized colloids with a softened core.

PACS numbers: 05.20.Jj, 61.20.Ja, 64.70.D-

In two dimensions thermal fluctuations do not allow the existence of a true crystalline order; in fact, only a quasi-long-range translational order is possible while bond-angular order is truly long-ranged. This opens the way to a two-stage melting transition through an intermediate “hexatic” phase with short-ranged translational order but extended bond-angle correlations. In the celebrated Kosterlitz-Thouless-Halperin-Nelson-Young (KTHNY) theory of two-dimensional (2d) melting [4], the hexatic phase is promoted by the thermal unbinding of dislocation pairs, followed by the proliferation of free disclinations on entering the normal fluid. The KTHNY theory predicts melting to be continuous. In two dimensions, when the energy of the dislocation core is sufficiently small, a first-order melting transition is more likely, driven by the spontaneous generation of grain boundaries [5, 6]. Hexatic phases have been observed in various types of colloids [7–15], and found also in some classical [16–20] and quantum simulations [21]. Moreover, nothing prevents the hexatic phase to be just metastable, as observed e.g. in Ref. [22].

Observing the KTHNY scenario is notoriously difficult because of the existence of important finite-size effects and long equilibration times. Also, the usually narrow temperature extent of the hexatic phase makes it hard to distinguish a two-stage melting from a single weakly first-order transition. Particularly severe is the situation for hard-core particles, where enormous samples and huge simulation times are required in order to discriminate between the various transition scenarios [23], while less demanding may be state sampling for systems of “soft” particles whose steric constraints are less pronounced.

We hereby inquire into the existence of a hexatic phase for the 2d Gaussian-core model (GCM) pair potential [24], $v(r) = \epsilon \exp(-r^2/\sigma^2)$ with $\epsilon > 0$, which is somewhat representative of a whole class of systems of interpenetrating particles (e.g. dilute dispersions of polymer chains) [25]. In three dimensions, this system is known to exhibit reentrant melting (*i.e.*, melting upon compression

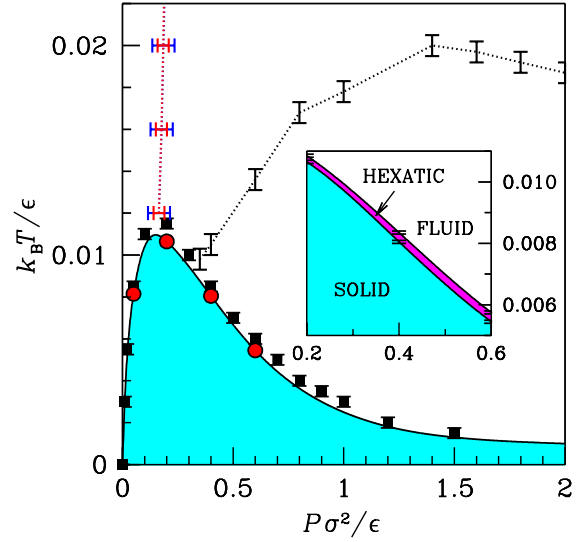


FIG. 1: (Color online). Phase diagram of the 2d GCM with anomaly loci. Plotted in black is the melting line, with red dots at the computed solid-to-hexatic transition points. The black squares (with error bars superimposed) give the upper stability threshold of the solid when heated isobarically in steps of $\Delta T = 0.0005$. The inset shows a magnified portion of the melting line with an adjacent (magenta) strip corresponding to the hexatic region. The dotted curves mark the boundary of anomaly regions (structural anomaly, red; diffusion anomaly, blue; density anomaly, black). Observe that the red and blue curves, which appear indistinguishable on the scale of the figure, depart from each other at much higher temperatures.

at constant temperature) [26] as well as waterlike anomalies [27]. Except for a 30-year old canonical-ensemble investigation [28] with inconclusive answers, we do not know of any simulation study of the melting behavior of 2d systems of particles with bounded interactions with a focus on the quest for a hexatic phase. Furthermore,

it would be interesting to know about the interplay between anomalous melting (that is, melting of the solid into an anomalous fluid) and the modality of decay of bond-angle correlations, an issue that has never been addressed before. As discussed in more detail below, the melting of the 2d GCM is indeed continuous and two-staged, with an extremely narrow hexatic region whose properties comply with the predictions of the KTHNY theory. The complete phase diagram is plotted in Fig. 1, together with a number of anomaly loci in the fluid phase.

Particles interacting through a repulsive Gaussian potential are expected to exhibit reentrant melting and a maximum melting temperature [29]. By examining all the five Bravais lattices and the honeycomb lattice, we first checked that the most stable state of the GCM at zero temperature is a triangular crystal for any pressure P . This gave us confidence that the triangular lattice provides the structure of the solid phase also for non-zero temperatures. We carried out isothermal-isobaric Monte Carlo (MC) simulations of N -particle samples (with N up to 6048) in order to locate melting for a number of selected pressures (0.05, 0.2, 0.4, and 0.6, in reduced, ϵ/σ^2 units). Our method consists in running simulations in a sequence, starting from the cold triangular solid on one side of the chain and from the hot fluid on the other side. Then, the solid was gradually heated (the fluid was cooled) in temperature steps of $\Delta T = 0.0005$ (in reduced, ϵ/k_B units), until we observed the abrupt melting (freezing) of the system. With this protocol, we found the same shape of the melting line as in the three-dimensional GCM, with a maximum melting temperature T_m of about 0.0115 for $P = P_m \lesssim 0.2$. We plot in Fig. 1 the melting line with three other curves which encompass regions in the fluid phase where an “anomalous” behavior occurs. On increasing the density, one first meets the so-called structural anomaly (which is where the absolute pair entropy reaches its maximum) [30], followed by the diffusion-anomaly locus (where the self-diffusion coefficient [31] attains its minimum), and by the density-anomaly line (where the particle-number density attains a local maximum). The same succession of anomaly loci is found in three dimensions [32].

To disentangle first-order from continuous melting, we performed another series of runs across our earlier guess of the transition point, now with a 5-time larger T resolution and also allowing for much longer equilibration times (10^6 sweeps, that is a million MC moves per particle) and production runs (5×10^6 sweeps). A typical result is shown in Fig. 2, where we report the average specific energy u and particle-number density ρ for various system sizes as a function of T for $P = 0.6$. A continuous path joins the solid and fluid branches with no evidence of hysteresis, which points to a smooth transition between the solid and fluid phases. Moreover, the energy and volume histograms have a simple Gaussian shape with no trace of bimodality within the relevant temperature range. As

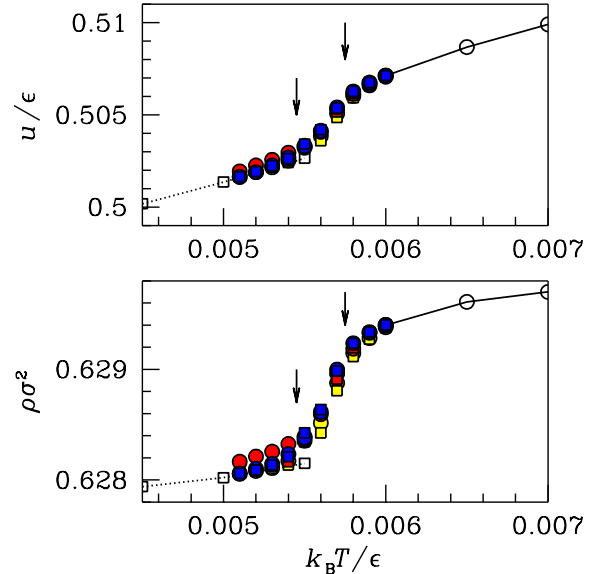


FIG. 2: (Color online). Total energy per particle (top) and particle-number density (bottom) for three different sizes ($N = 1152$, yellow; $N = 2688$, red; $N = 6048$, blue) for $P = 0.6$. We show results for both heating (squares) and cooling (dots) trajectories (one million MC sweeps of equilibration plus five million sweeps of data accumulation). The solid and fluid branches (dotted and solid lines, respectively) are computed with $N = 1152$ and much smaller statistics. The arrows mark the estimated transition points (see Fig. 3). The small hysteresis observed upon cooling for $N = 2688$ indicates that much longer runs are needed in order that the solidifying system may get rid of the extra defects.

we are going to show in the following, the intermediate region between the solid and the (normal) fluid can be qualified as hexatic.

We measured two different order parameters (OP), which are separately sensitive to the overall translational and orientational triangular order, with their respective susceptibilities and correlation functions. The translational OP is taken to be

$$\psi_T = \frac{1}{N} \left\langle \left| \sum_i e^{i\mathbf{G} \cdot \mathbf{r}_i} \right| \right\rangle, \quad (1)$$

where the sum is over the particle labels and \mathbf{G} is any first-shell reciprocal-lattice vector of the triangular crystal. From its very definition, it follows that ψ_T is sizeable only in a triangular solid that is oriented in a way consistent with the length and direction of \mathbf{G} . Hence, ψ_T is only measured on heating, where memory of the original crystal orientation is preserved as long as the system is large and remains solid. We anyway checked – through the location of the main peaks of the structure factor – that the orientation of the solid never changed from one run to the next. A sharp drop of ψ_T signals the melting of the solid into a fluid, be it hexatic or normal; concur-

rently, the corresponding susceptibility

$$\chi_T = \frac{1}{N} \left\langle \left| \sum_i e^{i\mathbf{G} \cdot \mathbf{r}_i} \right|^2 \right\rangle - N\psi_T^2, \quad (2)$$

shows a distinct peak whose location is an unambiguous estimate of the melting transition point. At regular intervals during the simulation, we made use of the Voronoi construction in order to identify the $n_c(i)$ nearest neighbors (NN) of each particle i , together with the orientation θ_{NN} of each neighbor bond with respect to a reference axis. Whence, the orientational OP follows as

$$\psi_6 = \frac{1}{N} \left\langle \left| \sum_i \frac{1}{n_c(i)} \sum_{NN(i)} e^{6i\theta_{NN}} \right| \right\rangle \equiv \frac{1}{N} \left\langle \left| \sum_i \Psi_6(\mathbf{r}_i) \right| \right\rangle. \quad (3)$$

The orientational susceptibility χ_6 is then defined in a way analogous to Eq. (2), with $\Psi_6(\mathbf{r}_i)$ replacing $\exp(i\mathbf{G} \cdot \mathbf{r}_i)$. ψ_6 undergoes a sudden drop at the hexatic-fluid transition, *i.e.*, at a temperature larger than the one where ψ_T vanishes. Finally, the local bond-angular OP $\Psi_6(\mathbf{r}_i)$ enters the definition of the orientational correlation function (OCF):

$$h_6(r) = \rho^{-2} \left\langle \sum'_{i,j} \delta^3(\mathbf{r}_i - \mathbf{R}) \delta^3(\mathbf{r}_j - \mathbf{R}') \Psi_6(\mathbf{r}_i) \Psi_6^*(\mathbf{r}_j) \right\rangle, \quad (4)$$

where the prime over the sum excludes $i = j$ and $r = |\mathbf{R} - \mathbf{R}'|$. The KTHNY theory predicts an algebraic $r^{-\eta(T)}$ large-distance decay of the OCF in the hexatic phase, which should be contrasted with the exponential asymptotic vanishing of angular correlations in a normal fluid. Another prediction of the theory is $\eta = 1/4$ at the hexatic-to-normal fluid transition point.

In Fig. 3, we plot the two OPs and susceptibilities for $P = 0.6$ (an analogous behavior was observed for all the other pressures). We see that ψ_T vanishes at a slightly smaller temperature than ψ_6 , which implies that the hexatic phase is confined to an extremely narrow T interval not wider than 0.0002–0.0003, as also witnessed by the maxima of the two susceptibilities occurring at slightly different T values. The estimated width of the hexatic region compares well with the temperature range of the bridging region between the solid and fluid branches in Fig. 2. While the size scaling of χ_6 is a clear imprint of a second-order hexatic-to-normal fluid transition, the solid-to-hexatic transition might even be first-order, were this not in contrast to the smooth behavior of u and ρ . Upon reducing the pressure, the width of the hexatic phase gradually shrinks until, for $P = 0.05$, it becomes comparable to the temperature resolution. However, even in this case we tend to exclude the disappearance of the hexatic phase for low pressures since this would imply the existence of a triple point for which we currently have no independent evidence. Finally, it is worth mentioning

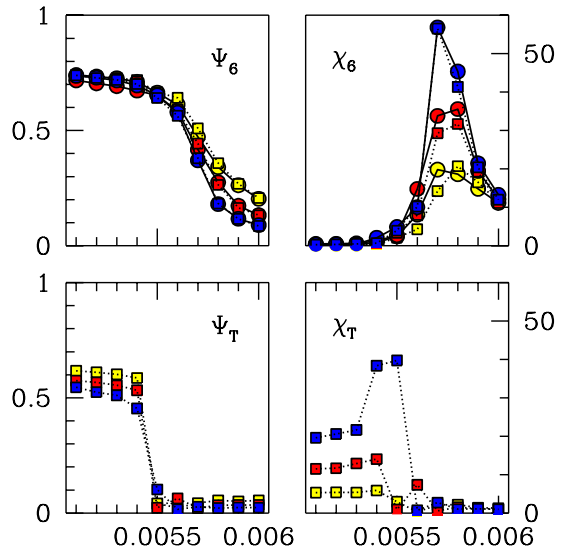


FIG. 3: (Color online). Order parameters and susceptibilities for $P = 0.6$ in the T range across the melting transition. Upper panels: the orientational order parameter ψ_6 and its susceptibility χ_6 for three system sizes (color codes as in Fig. 2). Dots and squares mark data obtained by cooling and by heating, respectively. Roughly, the difference between the two estimates gives a clue about the statistical uncertainty associated with each data point. Lower panels: the translational order parameter ψ_T and its susceptibility χ_T for the same sizes on heating. The non-zero value of ψ_T in the solid phase is actually a finite-size effect, made possible by the use of periodic boundary conditions in the simulations, since for a 2d *infinite* solid quasi-long-range translational order implies $\psi_T = 0$. Moreover, χ_T is expected to diverge in the solid phase of an infinite-size system. Similar considerations apply for the behavior of ψ_6 and χ_6 in the hexatic phase.

the case $P = 0.2$ (a pressure above P_m but outside the density-anomaly region), where the hexatic fluid shows a density anomaly while the normal fluid does not – in no other way could the density branch of the normal fluid have hooked on a solid branch that lies at a lower density level.

A more direct evidence of the hexatic phase emerges from the large-distance behavior of the OCF. We plot this function in Fig. 4 at various temperatures across the hexatic phase for $P = 0.6$. It appears that the OCF decays algebraically in a T region of limited extent, which roughly corresponds to the middle of the bridging region in Fig. 2. Moreover, the decay exponent in this hexatic region is smaller than $1/4$, becoming larger only on passing to the normal fluid.

We finally checked a further KTHNY prediction concerning the behavior of a 2d triangular solid which is about to melt into a hexatic phase. The elastic instability that signals the onset of dissociation of dislocation pairs, preluding to the stabilization of the hexatic phase,

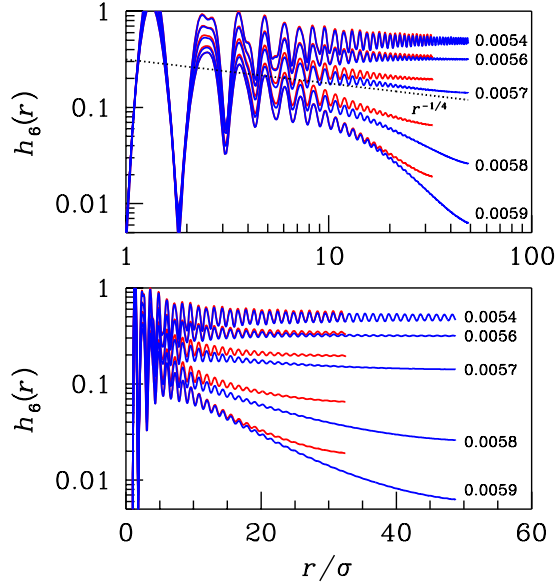


FIG. 4: (Color online). Oritational correlation function $h_6(r)$ at selected temperatures across the hexatic region for $P = 0.6$. We plot $h_6(r)$ on heating for two sizes, $N = 2688$ (red) and $N = 6048$ (blue). Top: log-log plot; bottom: log-lin plot. Upon increasing T from 0.0054 to 0.0059 there is a qualitative change in the large-distance behavior of $h_6(r)$, from constant (solid) to power-law decay (hexatic fluid), up to exponential decay (normal fluid). Note that, consistently with the KTHNY theory, the decay exponent η is less than $1/4$ (*i.e.*, the slope of the dotted curve) in the hexatic phase.

is heralded by the value of

$$K = \frac{4a^2}{k_B T} \frac{\mu(\mu + \lambda)}{2\mu + \lambda} \quad (5)$$

becoming equal to 16π [4, 33]. In Eq.(5), λ and μ are the Lamé coefficients (as renormalized by the thermal fluctuations) while $a = \sqrt{2/(\sqrt{3}\rho)}$ is the lattice parameter. λ and μ are respectively given by $c_{12} + P$ and $c_{44} - P$, in terms of the elastic constants c_{12} and c_{44} which can be computed as canonical-ensemble averages from virial-like formulae [34]. We found an impressive confirmation of the theory for $P = 0.6$ while the threshold value of $K/(16\pi)$ (before its drop to zero) turned out to be a bit larger than one (1.1–1.2) for the other investigated pressures. This further indicates that the overall KTHNY picture deteriorates with reducing pressure, probably because the formation energy of a dislocation becomes smaller and smaller with increasing average interparticle distances.

In conclusion, we have provided the first unambiguous evidence of the occurrence of two-stage continuous reentrant melting via a hexatic phase in the 2d Gaussian-core model, taken as prototypical of the phase behavior of bounded model potentials. We have validated a number of KTHNY predictions, though larger samples and

more statistics will be necessary in order to ascertain the real nature of melting at low densities. The present discovery of reentrant-hexatic behavior in the GCM is relevant for many soft-matter systems. For instance, one can engineer colloidal particles interacting through a temperature-modulated softened repulsion, which will likely exhibit GCM-like reentrant melting in a range of packing fractions well below the density at which hard-core crystallization occurs (see [35] for a 3d realization of this scenario). Such systems would be natural candidates where to detect (e.g. by video microscopy [36]) a reentrant-hexatic phenomenon of the kind illustrated here.

-
- [*] E-mail: Santi.Prestipino@unime.it
[†] Corresponding author. E-mail: saija@me.cnr.it
[‡] E-mail: Paolo.Giaquinta@unime.it
[4] J. M. Kosterlitz and D. J. Thouless, *J. Phys. C* **6**, 1181 (1973); B. I. Halperin and D. R. Nelson, *Phys. Rev. Lett.* **41**, 121 (1978); A. P. Young, *Phys. Rev. B* **19**, 1855 (1979).
[5] S. T. Chui, *Phys. Rev. B* **28**, 178 (1983).
[6] K. J. Strandburg, *Rev. Mod. Phys.* **60**, 161 (1988).
[7] C. A. Murray and D. H. Van Winkle, *Phys. Rev. Lett.* **58**, 1200 (1987).
[8] A. H. Marcus and S. A. Rice, *Phys. Rev. Lett.* **77**, 2577 (1996).
[9] K. Zahn, R. Lenke, and G. Maret, *Phys. Rev. Lett.* **82**, 2721 (1999).
[10] R. P. A. Dullens and W. K. Kegel, *Phys. Rev. Lett.* **92**, 195702 (2004).
[11] H. H. von Grünberg, P. Keim, K. Zahn, and G. Maret, *Phys. Rev. Lett.* **93**, 255703 (2004).
[12] P. Keim, G. Maret, and H. H. von Grünberg, *Phys. Rev. E* **75**, 031402 (2007).
[13] B.-J. Lin and L.-J. Chen, *J. Chem. Phys.* **126**, 034706 (2007).
[14] Y. Han, N. Y. Ha, A. M. Alsayed, and A. G. Yodh, *Phys. Rev. E* **77**, 041406 (2008).
[15] Y. Peng, Z. Wang, A. M. Alsayed, A. G. Yodh, and Y. Han, *Phys. Rev. Lett.* **104**, 205703 (2010).
[16] A. Jaster, *Phys. Rev. E* **59**, 2594 (1999).
[17] S. Muto and H. Aoki, *Phys. Rev. B* **59**, 14911 (1999).
[18] S. Z. Lin, B. Zheng, and S. Trimper, *Phys. Rev. E* **73**, 066106 (2006).
[19] S. I. Lee and S. J. Lee, *Phys. Rev. E* **78**, 041504 (2008).
[20] W.-K. Qi, Z. Wang, Y. Han, and Y. Chen, *J. Chem. Phys.* **133**, 234508 (2010).
[21] B. K. Clark, M. Casula, and D. M. Ceperley, *Phys. Rev. Lett.* **103**, 055701 (2009).
[22] K. Chen, T. Kaplan, and M. Mostoller, *Phys. Rev. Lett.* **74**, 4019 (1995).
[23] E. P. Bernard and W. Krauth, arXiv:1102.4094
[24] F. H. Stillinger, *J. Chem. Phys.* **65**, 3968 (1976).
[25] C. N. Likos, *Phys. Rep.* **348**, 267 (2001).
[26] See e.g. S. Prestipino, F. Saija, and P. V. Giaquinta, *Phys. Rev. E* **71**, 050102(R) (2005).
[27] See e.g. P. Mausbach and H.-O. May, *Fluid Phase Equilib.* **249**, 17 (2006).

- [28] F. H. Stillinger and T. Weber, *J. Chem. Phys.* **74**, 4015 (1981).
- [29] C. N. Likos, A. Lang, M. Watzlawek, and H. Löwen, *Phys. Rev. E* **63**, 031206 (2001).
- [30] P. V. Giaquinta and F. Saija, *Chem. Phys. Chem.* **6**, 1768 (2005).
- [31] The self-diffusion coefficient D was computed for $N = 1152$, via molecular dynamics, from the long-time behavior of the mean square displacement (MSD) of the particles; we found that the MSD increases linearly with time over a wide time interval and does not show any significant size dependence in the region explored.
- [32] W. P. Krekelberg, T. Kumar, J. Mittal, J. R. Errington, and T. M. Truskett, *Phys. Rev. E* **79**, 031203 (2009).
- [33] M. A. Bates and D. Frenkel, *Phys. Rev. E* **61**, 5223 (2000).
- [34] O. Farago and Y. Kantor, *Phys. Rev. E* **61**, 2478 (2000).
- [35] C. P. Royall, M. E. Leunissen, A.-P. Hynninen, M. Dijkstra, and A. van Blaaderen, *J. Chem. Phys.* **124**, 244706 (2006).
- [36] C. A. Murray and D. G. Grier, *Annu. Rev. Phys. Chem.* **47**, 421 (1996).